In-situ observation of phase transformation during laser welding processes†

YAMADA Tomonori*, YONEMOTO Yukihiro*, YAMASHITA Susumu*,
MURAMATSU Toshiharu* and KOMIZO Yu-ichi **

KEY WORDS: (Laser welding) (Weld metal) (In-situ observation) (Nucleation site)

1. Introduction

It is known that residual stress is important to keep structural integrity. Laser welding is effective for a residual stress decrease because heat input is smaller and have a less effect. Therefore, repair technology by laser welding has drawn wide attention for the life extension of FBRs (Fast Breeder Reactors). To establish laser repair technology, special attentions should be paid to the morphological developments.

In the present work, morphological developments were directly observed using laser scanning confocal microscopy during laser weld cooling.

2. Experiments

The tested materials were low carbon Ti-B weld metals with an oxygen content of 460ppm and machined into sample discs for observation. **Table 1** shows the chemical compositions of the weld metals used. The compositions of inclusions were varied by changing aluminium content while the contents of the other elements kept constant. The Al/O ratios (mass ratio) were 0.48, 0.73 and 1.52.

Table1 Chemical compositions of weld metals used(mass%).

	C	Si	Mn	Ti	B	O	N	Al
Y1	0.090	0.35	1.72	0.014	0.0035	0.046	0.0042	0.022
Y2	0.085	0.37	1.75	0.015	0.0040	0.048	0.0041	0.035
Y3	0.086	0.39	1.81	0.013	0.0040	0.048	0.0035	0.073

For in situ observation of phase transformation during thermal cycle of laser welding, a high temperature laser scanning microscope (HLSCM) system was used. This system consists of LSCM and infrared image furnace (IIF).

The sample disc was machined to 5mm diameter and 1mm in height and the observed plane was mirror polished. The sample in the high purity alumina crucible was set on the platinum holder connected to a B type thermocouple. **Figure 1** shows schematic illustration for the sample holder in an infrared image furnace and the optical system. The high scanning rate (30frame rates) is due to the acoustic optical deflector and only the focal point can be detected by the CCD camera without the effects of high temperature radiation since a confocal optical system is used. The atmosphere was filled with high purity argon shielding gas (99.9999%) after evacuating to 1×10^{-2}Pa[1]. In the present work, the following thermal cycle was applied to the samples. To make the austenite grain diameter uniform, heating rate was 13.3°C/sec to 1400°C. Cooling rate was 5°C /sec between 1400°C and 800°C. To assume the cooling rate of the laser welding, the sample was cooled by the maximal rate (54.5°C/sec) from 800°C.

To clarify the microstructural evolution mechanism, the inclusions were investigated from the crystallographic point of view. The foil samples including inclusions were prepared in a focused ion beam (FIB) device and were observed by a transmission electron microscope (TEM) in which the accelerated voltage of 200kV was used.

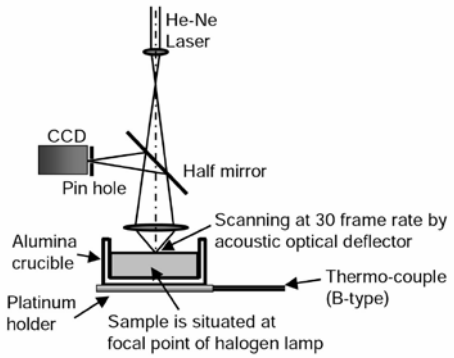

Fig. 1 Schematic illustration for optical system in high temperature laser scanning confocal microscopy.

3. Results and Discussion

Figure 2 shows the results of in-situ morphological development observation of transformation for Y2 (Al/O=0.73). When sample was cooled to 596°C, transformation to ferrite from near the inclusions in the austenite grains was observed. The circle shows morphological change corresponding to acicular ferrite growing. It was clear that morphological change corresponding to acicular ferrite growing. It was clear that the morphological change corresponding to phase transformation. This result shows that the grain boundary did not operate as a nucleation site. When sample was cooled to 441°C, transformation was finished. Therefore, the interface between nucleation site (inclusion) and ferrite

† Received on 30 September 2010
* Japan Atomic Energy Agency
** JWRI, Osaka University, Ibaraki, Japan
Transactions of JWRI is published by Joining and Welding Research Institute, Osaka University, Ibaraki, Osaka 567-0047, Japan

was observed.

Figure 3 shows the HAADF-STEM image, EDS mapping analysis, EDS spectrum and selected area diffraction pattern from inclusions in Y2 in which acicular ferrite was observed. This inclusion was surrounded by a titanium enriched layer. This layer was identified as TiO by EDS spectrum and SAD. The TiO has a Baker-Nutting orientation with acicular ferrite. In this case, the lattice misfit between TiO and acicular ferrite is 3.0%[2]. Therefore, the TiO on the inclusion surface promotes intragranular nucleation supplying low interface energy.

Figure 4 shows the corresponding crystal-orientation maps measured in the Y2(Al/O=0.73) by EBSD analysis. Inverse pole figure color maps show the distributions of ferrite and austenite, respectively. The pole figure of ferrite shows {110} and {111}. Moreover, the pole figure of austenite shows {111} and {101}. From these pole figure, $\{110\}_{\alpha Fe}$ and $\{111\}_{\gamma Fe}$, $\{111\}_{\alpha Fe}$ and $\{101\}_{\gamma Fe}$ were parallel, respectively. Therefore, these results suggest that they have Kurdjumov-Sachs (K-S) orientation relationship.

Figure 5 shows the schematic illustration for orientation relationship between TiO and acicular ferrite, orientation relationship between acicular ferrite and austenite. The inclusions which related to acicular ferrite formation were surrounded by TiO. The B-N orientation relationship was satisfied between the TiO and acicular ferrite. The K-S orientation relationship was satisfied between the acicular ferrite and austenite. Therefore, a crystal plane of acicular ferrite corresponds to the habit plane $\{111\}_{\gamma Fe}$ and the growth direction was $<111>_{\alpha Fe}$.

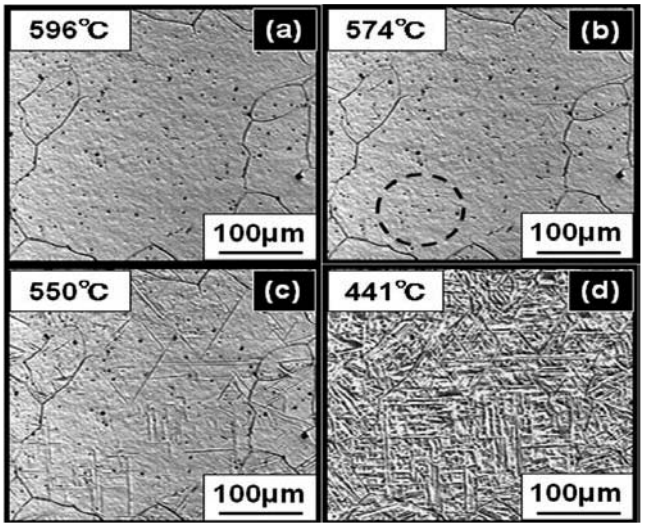

Fig. 2 In-situ observation of morphological development in Y2(Al/O=0.73). (a)596°C ; (b)574°C ; (c)550°C ; (d)441°C.

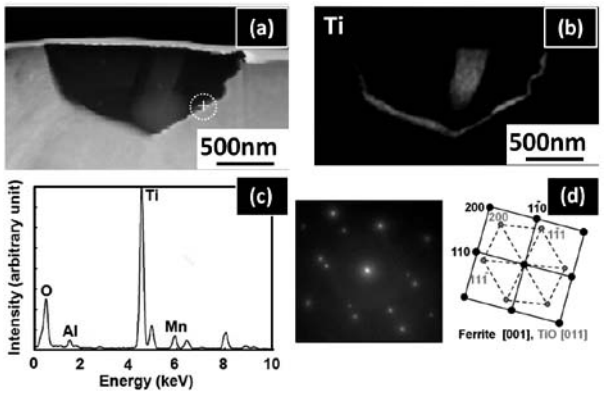

Fig. 3 TEM analysis of inclusion after thermal cycle in Y2(Al/O=0.73). (a)HAADF-STEM image ; (b)EDS mapping by Ti-K_{α} X-ray ; (c)EDS spectrum from the point indicated by a cross in the HADDF image; (d) Selected area diffraction pattern from the area indicated by a circle in the HADDF image and its key diagram.

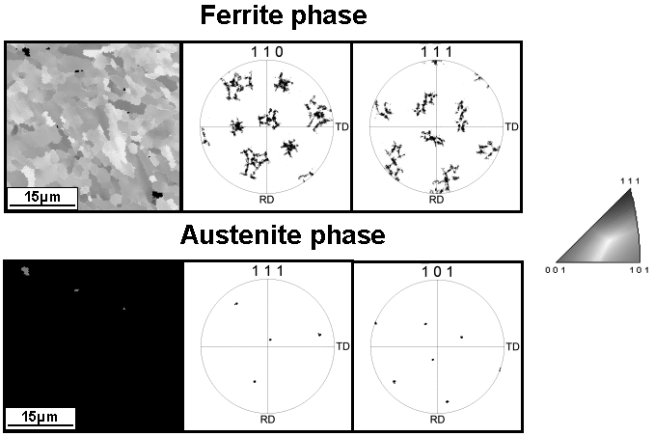

Fig. 4 The corresponding crystal-orientation map measured in the Y2(Al/O=0.73) by EBSD analysis.

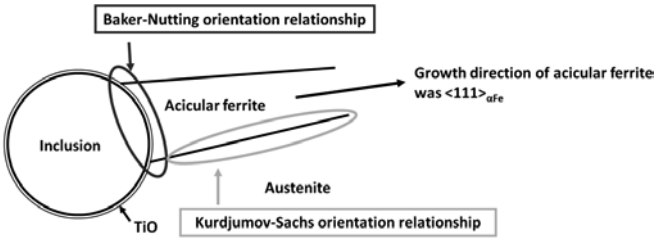

Fig. 5 Schematic illustration for metallurgical phenomena around inclusion.

4. Conclusions

The phase transformation was observed in-situ during laser weld cooling in low carbon Ti-B weld metals with three levels of Al/O ratio. The findings obtained in the present research are as follows.

(1) Acicular ferrite nucleated intragranularly on inclusions within the austenite grains in weld metals with low and medium Al/O ratio.

(2) The inclusions which related to acicular ferrite formation were surrounded by a TiO layer.
(3) The Baker-Nutting orientation relationship was satisfied between the TiO layer and acicular ferrite.
(4) It was suggested that the TiO on the inclusion surface contributes to the heterogeneous nucleation of acicular ferrite, supplying low interface energy.

References

[1] H.Terasaki and Y.Komizo: Sci. Technol. Weld. Joining, 11(2006), pp.561–566.

[2] T.Yamada, H.Terasaki and Y.Komizo: Tetsu-to-Hagane, 95(2009), pp.65-70.